

Polyphosphazene Membranes. IV. Polymer Morphology and Proton Conductivity in Sulfonated Poly[bis(3-methylphenoxy)phosphazene] Films

HAO TANG, PETER N. PINTAURO¹

Department of Chemical Engineering, Tulane University, New Orleans, Louisiana 70118

Received 30 July 1999; accepted 1 March 2000

ABSTRACT: The microstructure of sulfonated poly[bis(3-methylphenoxy)phosphazene] was studied using wide- and small-angle X-ray diffraction. A reflection peak, attributed to the presence of ionic clusters, was observed in the small-angle X-ray diffraction patterns of hydrated and dry polymers with an ion-exchange capacity (IEC) ≥ 0.6 mmol/g. The Bragg spacing from the ionic cluster structure was about 30 Å for the nonhydrated polymer and 50 to 90 Å for fully hydrated films. The effects of IEC, cation form of the polymer, temperature, and polymer water content on the cluster structure were investigated. The specific proton conductivity of water-swollen, sulfonated poly[bis(3-methylphenoxy)phosphazene] films at 25°C increased with increasing IEC, with a maximum conductivity of 0.1 S/cm at a polymer ion-exchange capacity of 1.6 mmol/g. The water-content percolation threshold for conductivity was between 17.5 and 25 vol %, and decreased with polymer IEC. The temperature dependence of proton conductivity for 1.2 mmol/g IEC poly[bis(3-methylphenoxy)phosphazene] membranes exhibited Arrhenius behavior with an apparent activation energy of 27.8 and 36.7 kJ/mol for crosslinked and noncrosslinked polymers, respectively. © 2000 John Wiley & Sons, Inc. *J Appl Polym Sci* 79: 49–59, 2001

Key words: polyphosphazene; ion-exchange membrane; small-angle X-ray scattering; cluster structure; proton conductivity

INTRODUCTION

Perhaps the most important property of an ionomeric membrane, from an applied electrochemical point of view, is its ionic conductivity, especially for a water-swollen film. Perfluorosulfonic acid ion-exchange membranes, such as Nafion[®] from DuPont de Nemours & Co., Inc., and

Flemion[®] from Asahi Glass Co., for example, have been used in a variety of electrochemical processes and devices such as chlor-alkali cells,¹ battery separators,² and fuel cells³ due, in large part, to their high proton/cation conductivity. Ion conductivity in these polymers is closely related to the internal polymer structure, in particular the spatial distribution of fixed-charge sites and the degree of polymer swelling by water.

During sorption of a polar solvent such as water, the hydrophilic ion-exchange groups of an ionomeric polymer tend to separate from the hydrophobic matrix and form aggregates, due to electrostatic interactions between fixed-charge sites and mobile counterions. The most direct evidence for the existence of fixed-charge site aggrega-

Correspondence to: P. N. Pintauro (peter.pintauro@tulane.edu).

Contract grant sponsor: Army Research Office; Contract grant number: 38973-CH.

Contract grant sponsor: National Science Foundation; Contract grant number: CTS-9632079.

Journal of Applied Polymer Science, Vol. 79, 49–59 (2001)
© 2000 John Wiley & Sons, Inc.

gation is the appearance of a peak in the small-angle X-ray scattering (SAXS) pattern of hydrated ionomeric films. To explain these SAXS observations, several microstructure models have been proposed for fixed charge aggregation, such as: (1) The core-shell model,⁴ where ionic clusters are shielded from the surrounding polymer matrix by a shell of hydrocarbon chains and where the observed scattering maximum arises from intraparticle interference of the core-shell aggregates, reflecting a short-range order distance associated with the size of the core and shell; (2) the two-phase model,⁵ where small fixed-charge aggregates are assumed to be distributed uniformly throughout the polymer and where the X-ray scattering maximum is attributed to interparticle interference, which is related to the regularly repeating intercluster distance; and (3) the local order model,⁶ where ionic clusters create a quasi-crystal order in the ionomer, the organization of which is affected by the presence of low-mobility chains and where the clusters themselves are ordered in a hypercrystal with a large-cell size.

Using SAXS data and one of the models presented above, researchers over the years have proposed a variety of different microstructure portraits for dry and solvent-swollen Nafion membranes; for example, Fujimura⁷ (the core-shell model for electrolyte-swollen membranes), Gierke et al.⁸ (spherical clusters on a simple two-phase cubic lattice network), and Gebel et al.⁹ (who found that their data compared well with those deduced from the local order model). Of course, the real interest in developing a microstructure model for solvent-swollen ion-exchange membranes is to relate the polymer morphology to macroscopic membrane transport properties. For Nafion materials, researchers have had some success in relating coion uptake and transport to the cluster-network model of Gierke.¹⁰

The purpose of the present study was to investigate the microstructure and proton conductivity of sulfonated membranes composed of a phosphazene polymer, poly[bis(3-methylphenoxy)phosphazene] (henceforth abbreviated as PBMP), in the dry and water-swollen states. In our previous studies,^{11,12} well-formed, water-insoluble membranes, with an ion-exchange capacity (IEC) ranging from 0.6 to 1.6 mmol/g, were prepared from poly[bis(3-methylphenoxy)phosphazene]. The polymer was sulfonated in solution with SO₃ prior to film casting. In some cases, a crosslinking photoinitiator (benzophenone) was dissolved in the casting solution and C—C crosslinks between

polymer chains were created by exposing the film (after solvent evaporation) to UV light.^{13,14} Such crosslinking provided a means of independently controlling the ion-exchange capacity of the membranes and the degree of polymer swelling by water. Water-swollen PBMP ion-exchange membranes exhibited an interesting and highly desirable combination of transport properties for electrochemical (e.g., fuel cell) applications, namely a high proton conductivity with a low water diffusivity.¹²

EXPERIMENTAL

Materials and Procedures for Preparation of Polymer Membranes

Poly[bis(3-methylphenoxy)phosphazene] (PBMP), purchased from “technically” Inc., Woburn, MA, was used as the base polymer without further purification. The molecular weight of the PBMP polymer, as determined by gel permeation chromatography (Waters Styragel HT 6E column in THF), was 2.0×10^6 daltons.

The phosphazene polymer was dissolved in dichloroethane and sulfonated with SO₃. The polymer was then pretreated by soaking sequentially in water, a dilute NaOH solution, water, and dilute acid over a period of 6 days and cast into a thin film from a 3 wt/vol % *N,N*-dimethylacetamide (DMAc) solution as described elsewhere.¹¹ Crosslinked polyphosphazene membranes were solution cast from the sulfonated polymer/DMAc solution with 15 mol % benzophenone (BP) as the photoinitiator. Fully dried films were exposed to 365-nm wavelength UV light (2.8 mW/cm² intensity) for 20 h. Sulfonated films in different salt forms (Li⁺, Na⁺, and Cs⁺) were obtained by soaking membrane samples in a 2.0 M LiCl, NaCl, or CsCl solution for 48 h, followed by a 24-h membrane soak in deionized/distilled water.

The ion-exchange capacity (denoted as IEC, with units of mmol/g of dry polymer) of the sulfonated PBMP membranes was measured using the standard experimental method of immersing the membrane in acid (to ensure that all counterions associated with SO₃⁻ fixed-charge groups were protons) followed by soaking in distilled water (to remove excess acid), soaking in 2.0 M NaCl solution (to exchange Na⁺ for H⁺ within the film), and then titrating the salt solution with NaOH to determine the concentration of desorbed H⁺.

Equilibrium water uptake (swelling) was quantified in terms of the % increase in weight (W) and the % increase in volume (ΔV) of membrane samples, according to the formulas:

$$W = \frac{m_{\text{wet}} - m_{\text{dry}}}{m_{\text{dry}}} \times 100 \text{ and } \Delta V = \rho_p W \quad (1)$$

where m_{wet} and m_{dry} are the weights of the same water-swollen and dry membrane sample, respectively, and ρ_p is the dry polymer density.

Membrane Characterization

Wide-angle X-ray diffraction (WAXD) patterns were obtained using a Rigaku Model RU200B diffractometer that was operated at 55 kV and 190 mA with a nickel-filtered Cu-K $_{\alpha}$ ($\lambda = 1.54 \text{ \AA}$) X-ray beam. Diffraction data were collected from dry and water-swollen films, that were placed in sealed glass tubes. The scan rate was $2.0^\circ/\text{min}$, and the temperature was controlled to within $\pm 1.0^\circ\text{C}$ by a custom-made electrical heating device.

Small-angle X-ray scattering (SAXS) measurements at different temperatures were collected with a Rigaku 12-KW rotating anode diffractometer, using Ni-filtered Cu-K $_{\alpha}$ radiation and a Rigaku scintillation counter detector. The temperature was controlled by a custom-made electrical heating device. The beam was collimated by two slits of widths 0.16 and 0.12 mm. The sample-to-detector distance was 200 mm and the scanning rate was $0.01^\circ/\text{min}$. To obtain small-angle X-ray diffraction data on partially and fully hydrated samples, polymer films were sealed thermally in a bag composed of oriented polypropylene, which was essentially transparent to the small-angle X-ray beam and possessed a very low water vapor permeability. With such a device, it was found that the weight of a water-swollen membrane changed by less than 0.5% during the time period required to obtain a small-angle X-ray scan.

The electrical conductivity of protons in water-equilibrated and sulfonated PBMP membranes in the H $^+$ form was determined using an AC impedance method. Conductivity in the longitudinal (XY) plane was measured using a pair of pressure-attached, high surface area platinum electrodes, as described elsewhere.¹⁵ For fully hydrated membranes, the mounted sample was immersed in deionized and distilled water at a given

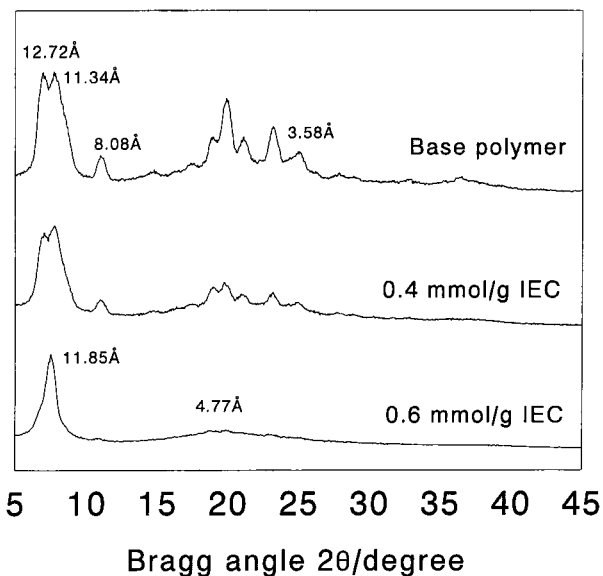


Figure 1 Wide-angle X-ray diffractograms from dry (nonhydrated) poly[bis(3-methylphenoxy)phosphazene] at 25°C .

temperature. For partially hydrated membranes, the sample film was first equilibrated in deionized and distilled water and then air dried until the desired degree of water swelling was achieved. The sample was mounted in the conductivity cell, which was then enclosed in a polypropylene bag to prevent further water loss. The conductivity measurements were made with AC currents ranging in frequency from 1.0 Hz to 10^5 Hz using a PAR Model 5210 amplifier and a PAR Model 273 potentiostat/galvanostat. Both real and imaginary components of the impedance were measured and the real Z-axis intercept was closely approximated. The cell constant was calculated from the spacing of the electrodes and the membrane cross-sectional area (the thickness and width of the membrane).

RESULTS AND DISCUSSION

Wide-Angle X-ray Diffraction

X-ray diffractograms of the PBMP polymer prior to and after sulfonation (with an IEC of 0.4 and 0.6 mmol/g) are shown in Figure 1. The base polymer was found to be semicrystalline, with two main reflection peaks at 12.72 and 11.34 \AA and several other reflections centered between 8.08 and 3.58 \AA . For the sulfonated polymer with an IEC 0.4 mmol/g, all of the base-polymer diffrac-

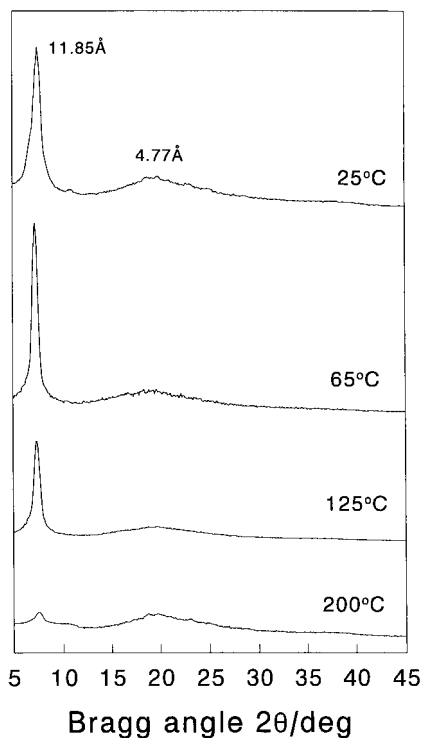


Figure 2 Wide-angle X-ray diffractograms of dry poly[bis(3-methylphenoxy)phosphazene] (sulfonated to an IEC of 1.2 mmol/g) recorded at different temperatures.

tion peaks were preserved, indicating that the main crystal structure of the phosphazene polymer was retained, although the intensity of the peaks between 8.08 and 3.58 Å was reduced. At a higher IEC (0.6 mmol/g), all diffraction peaks between 8.08 and 3.58 Å smeared out into an amorphous hole centered at 4.77 Å, but the main peak centered at 11.85 Å was still present (similar diffractograms were obtained with sulfonated polymers where the IEC was greater than 0.6 mmol/g). These results indicate that the polymer lost its three-dimensional crystal structure after a sufficient degree of sulfonation but a two-dimensional (2D) ordered phase was retained (the X-ray peak at 11.85 Å was identified as an intermolecular reflection peak¹¹).

The effect of temperature on the X-ray diffractograms for a 1.2 mmol/g PBMP sulfonated polymer is shown in Figure 2. The intensity of the main reflection peak at 11.85 Å increased significantly when the temperature was raised from 25 to 65°C, with a small decrease in the intensity of the amorphous hole at 4.77 Å, indicating an increase in 2D ordering with temperature. The intensity of the main peak decreased at 125°C and

nearly disappeared at 200°C, suggesting a gradual loss in the 2D structure at these two temperatures.

The influence of sorbed water on the X-ray diffractograms of a sulfonated (noncrosslinked) 1.2 mmol/g phosphazene polymer film is shown in Figure 3. The intensity of the main X-ray peak at 11.85 Å decreased with increasing membrane water content, while the amorphous hole at 4.77 Å remained unchanged. Although water molecules were absorbed into amorphous polymer domains, the WAXD results show that their presence in the polymer disturbed some of the crystal boundaries and decreased the 2D polymer crystallinity, presumably due to strong ion-ion interactions between hydrated sulfonic acid groups.

Small-Angle X-ray Scattering (SAXS)

SAXS Data from Dry (Nonhydrated) Membranes

Small-angle invariant X-ray scans from dry PBMP polymers (sulfonated but not crosslinked) with IECs ranging from 0.5–1.6 mmol/g are shown in Figure 4. When the ion-exchange capacity was ≥ 0.6 mmol/g, a reflection peak appeared in the scan. The peak intensity increased with IEC, but the apparent Bragg spacing of the reflection was essentially constant at about 30 Å (except for the 0.6 mmol/g IEC polymer, with a spacing of 24 Å).

Figure 5 shows the SAXS scans from a dry 1.2 mmol/g sulfonated PBMP film (noncrosslinked) in different counterion (cation) forms. The apparent Bragg spacing decreased in the order

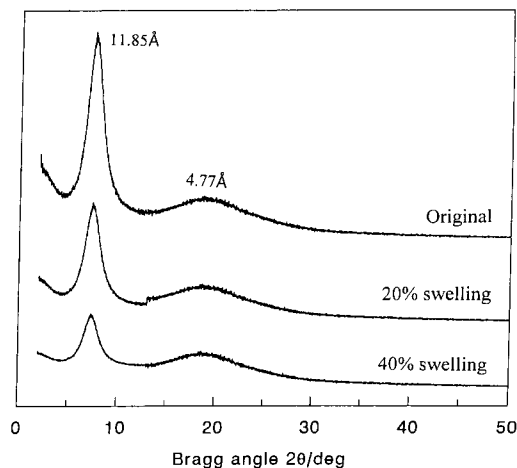


Figure 3 Wide-angle X-ray diffractograms of poly[bis(3-methylphenoxy)phosphazene] (1.2 mmol/g) at different degrees of water swelling (swelling in wt %).

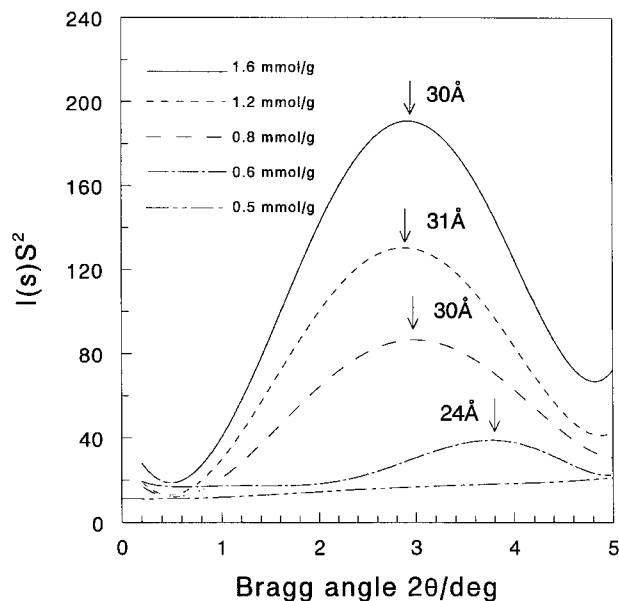


Figure 4 Small-angle invariant X-ray scans of sulfonated poly[bis(3-methylphenoxy)phosphazene] in dry (nonhydrated) film form with different polymer ion-exchange capacities.

$$\text{Cs}^+ \text{ form} > \text{Na}^+ \text{ form} > \text{Li}^+ \text{ form} > \text{form H}^+$$

i.e., the spacing decreased with decreasing molecular weight of the counterion associated with the

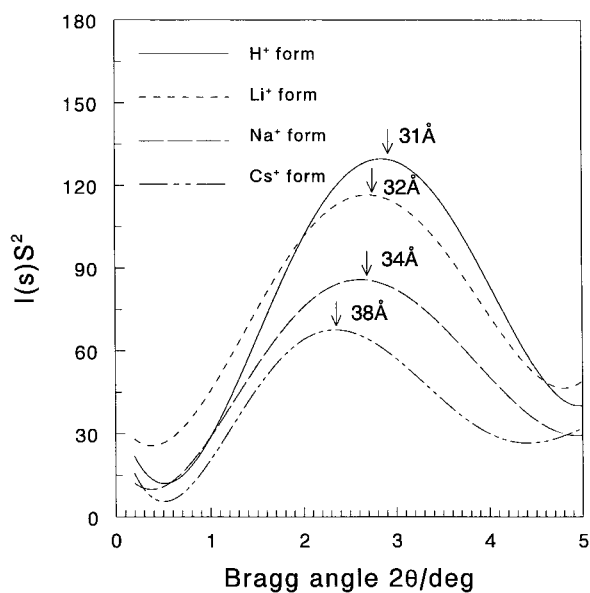


Figure 5 Effect of membrane salt form on small-angle invariant X-ray scans for dry (nonhydrated) poly[bis(3-methylphenoxy)phosphazene] at an IEC of 1.2 mmol/g.

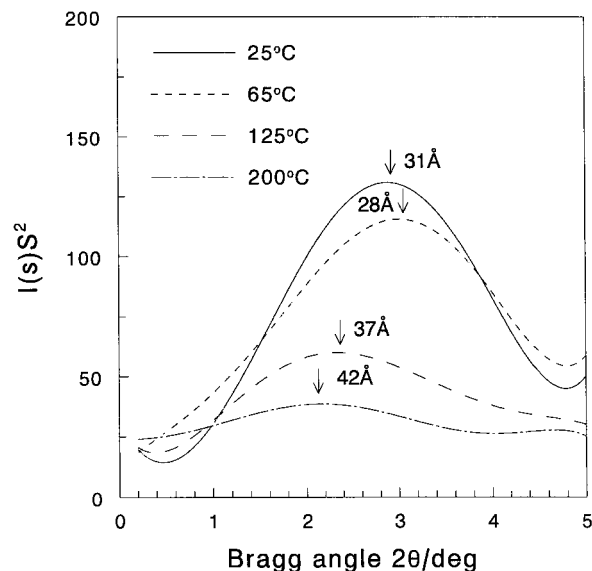


Figure 6 Small-angle invariant X-ray scans from dry (nonhydrated) poly[bis(3-methylphenoxy)phosphazene] at different temperatures (membrane in the H^+ form with an IEC of 1.2 mmol/g).

SO_3^- sites. The reflection intensity, on the other hand, exhibited the opposite trend with respect to the counterion. Regardless of whether the Bragg spacing is associated with an intercluster distance (according to the two-phase model) or an intracenter distance (according to core-shell model), the observed increase in Bragg spacing with counterion size was attributed to an increase in ion cluster size. The ability to form ionic clusters in sulfonated polymers through electrostatic interactions between SO_3^- and M^+ moieties is known to vary in the order $\text{SO}_3\text{H} < \text{SO}_3\text{Li} < \text{SO}_3\text{Na} < \text{SO}_3\text{Cs}$.¹⁶ It appears that a similar situation exists in the PBMP membranes.

The effect of temperature on the invariant SAXS scans of a dry 1.2 mmol/g PBMP membrane (in the H^+ counterion form) is shown in Figure 6. When the polymer was heated from 25 to 65°C, the reflection peak shifted to a higher angle, corresponding to a decrease in Bragg spacing from 31 to 28 Å. When the sample temperature was raised further to 125°C and then to 200°C, the Bragg angle decreased, indicating an increase in Bragg spacing to 37 Å at 125°C and to 42 Å at 200°C. The reflection intensity decreased with temperature, especially for $T \geq 125^\circ\text{C}$. By comparing the WAXD results in Figure 2 with the SAXS data in Figure 6, we can conclude that the size of ionic clusters in amorphous regions of the PBMP polymer is inversely related to the degree

Table I Bragg Spacing (with Units of Å) in Dry Films Composed of Crosslinked and Noncrosslinked Sulfonated Poly[bis(3-methylphenoxy)phosphazene] with Different Ion-Exchange Capacities

Polymer IEC (mmol/g)	0.6	0.8	1.0	1.2	1.4	1.6
Noncrosslinked films	24	30	31	31	31	30
Crosslinked films	26	33	35	38	39	42

of 2D polymer crystallinity and, thus, is directly related to the flexibility of the polymer chains. Although the crystallinity of the sulfonated PBMP polymer was essentially nonexistent at 200°C (see Fig. 2), a reflection maximum in the corresponding SAXS scan was still observable, which shows that the ionic clusters are more stable thermally than the 3D or 2D structure of the dry polymer. We have attributed this finding to the strong interactions between SO₃H fixed-charge sites.

The Bragg spacings in dry crosslinked and noncrosslinked sulfonated polymers with an IEC between 0.6 and 1.6 mmol/g are listed in Table I. The data show that the Bragg spacing of a crosslinked polymer at a particular IEC was slightly larger than that of its noncrosslinked counterpart. This result was attributed to the presence of unreacted benzophenone photoinitiator and benzopinacol molecules (a product of the UV crosslinking reaction with benzophenone photoinitiator) that acted as plasticizers and slightly decreased the polymer crystallinity, which in turn, made the cluster size larger in the crosslinked films, as compared to that in a noncrosslinked polymer of the same IEC.

SAXS Results from Hydrated Polymer Films

SAXS scans of fully hydrated PBMP polymer films with different IECs in the H⁺ form are shown in Figure 7. Unlike the SAXS results from dry polymer samples, the scattering maximum of hydrated films shifted towards smaller angles and the scattering intensity increased with increasing IEC. The Bragg spacing of the hydrated membranes was 63, 70, 80, and 92 Å for polymers with an IEC of 0.6, 0.8, 1.2, and 1.6 mmol/g, respectively. As was shown previously,¹¹ water uptake in sulfonated polyphosphazene mem-

branes increased with IEC and the Bragg spacing data suggests that this water absorbs into and expands ionic clusters. At the same time, the increase in cluster water content created an increase in the electron density difference of the clusters compared to the surrounding uncharged polymer, which produced the observed increase in reflection intensity with IEC.

The effect of ion-exchange capacity on the Bragg spacing for fully hydrated, crosslinked and noncrosslinked PBMP polymers is shown in Figure 8. As expected, the Bragg spacing increased with IEC for both crosslinking and noncrosslinking polymers, and decreased after polymer crosslinking for a given IEC (due to the reduced water swelling of the crosslinked films). SAXS scans of water-equilibrated (noncrosslinked) PBMP membranes in different counterion form are shown in Figure 9. The location of the reflection maximum and peak intensity for membranes in the H⁺ and Li⁺ forms were nearly identical. For the SO₃Na and SO₃Cs membranes, however, the reflection peak shifted towards higher angles with an accompanying decrease in peak intensity. The decrease in reflection intensity for membranes with heavier (larger) cations was a result of the increase in electron density of the cluster, which produced less contrast for X-ray scattering between the ionic clusters and polyphosphazene matrix. At the same time, the decrease in Bragg spacing was a result of the decrease in macro-

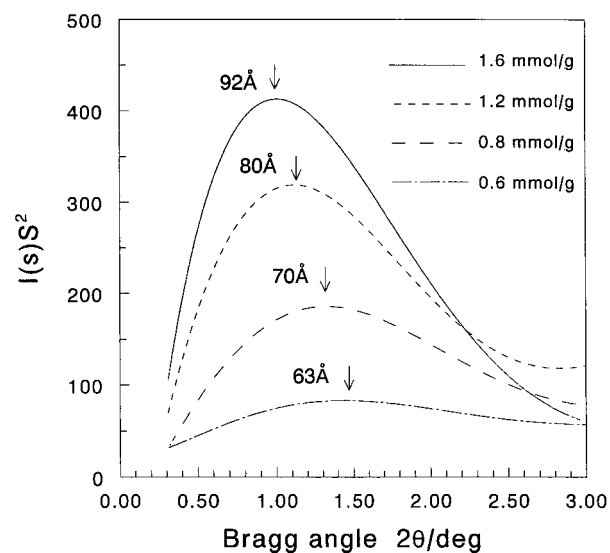


Figure 7 Effect of ion-exchange capacity on the small-angle invariant X-ray scans for hydrated poly[bis(3-methylphenoxy)phosphazene] ion-exchange membranes in the H⁺ form.

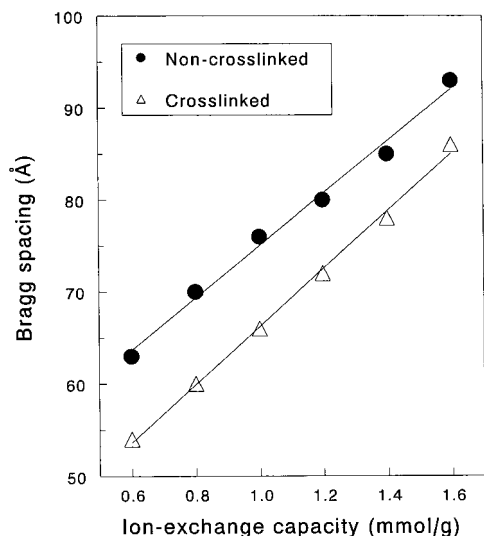


Figure 8 Variation in small-angle Bragg spacing with IEC for fully hydrated (water swollen) crosslinked and noncrosslinked membranes composed of sulfonated poly[bis(3-methylphenoxy)phosphazene] (all membranes in the H^+ form).

scopic water swelling, where swelling for the 1.2 mmol/g IEC films was 40, 38, 33, and 30% for membranes in the H^+ , Li^+ , Na^+ , and Cs^+ forms, respectively. It should be noted that although Nafion membranes exhibited the same qualitative water-swelling trend with counterion form as the PBMP films, the Bragg spacings of hydrated Nafion showed no correlation with polymer swelling.¹⁷

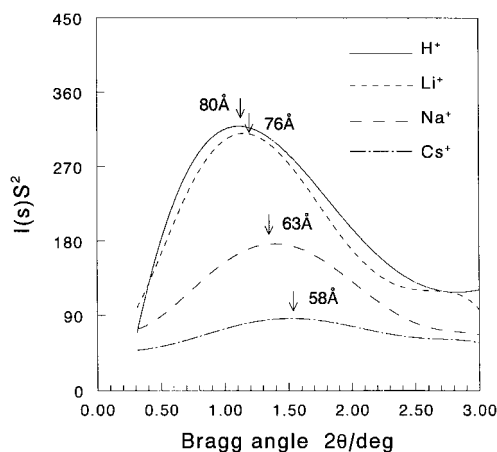


Figure 9 Small-angle invariant X-ray scans from fully hydrated, noncrosslinked, 1.2 mmol/g membranes composed of poly[bis(3-methylphenoxy)phosphazene] in different cation forms.

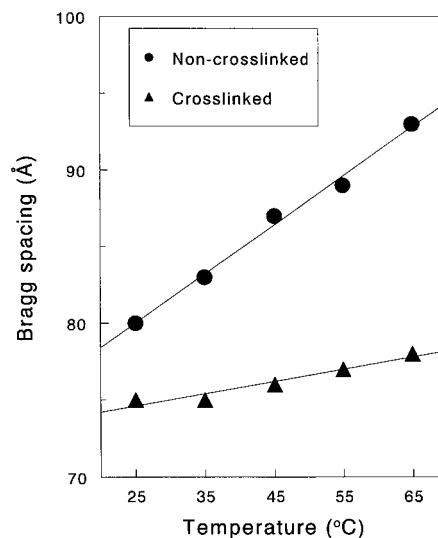


Figure 10 Variation of Bragg spacing with temperature for fully hydrated 1.2 mmol/g IEC, noncrosslinked and crosslinked (15 wt % benzophenone) poly[bis(3-methylphenoxy)phosphazene] membranes.

The effect of temperature on the Bragg spacing in noncrosslinked and crosslinked (15% benzophenone) 1.2 mmol/g sulfonated PBMP membranes in a fully hydrated state is shown in Figure 10. Here, membrane samples were soaked in pure water at a specific temperature between 25 and 65 °C for 24 h and then sealed in an oriented polypropylene bag to perform the SAXS experiment at the same temperature. The Bragg spacing increased with temperature for both membranes, but cluster size was more temperature dependent in the noncrosslinked membrane, which is consistent with our prior observations that C—C crosslinks in polyphosphazene films restricted polymer swelling and increased the polymer's glass transition temperature.

Microstructure Model of Clusters in Sulfonated PBMP Membranes

SAXS data from water-swollen PBMP ion-exchange membranes were interpreted using the Nafion “cluster-network” model of Gierke et al.,^{8,17} where the average size of the (assumed) spherical ionic clusters was related to the macroscopic membrane porosity and the Bragg spacing by,

$$D = \left[\frac{6d^3\Delta V}{\pi(1 + \Delta V)} + \frac{6N_p V_p}{\pi} \right]^{1/3} \quad (2)$$

where D is the cluster diameter; d is the distance between clusters (the Bragg spacing); ΔV is the

Table II Cluster Dimensions and Related Microstructure Parameters for Sulfonated (Noncrosslinked) PBMP Membranes of Different Ion-Exchange Capacities and in a Fully Hydrated State (Temperature = 25°C)

IEC (mmol/g)	ρ_p^a (g/cm ³)	Mass Gain, W (%)	Volume Gain, ΔV (%)	H ₂ O/SO ₃ H	H ₂ O/Cluster	Charge/Cluster	Bragg Spacing (Å)	Cluster Diameter (Å)
1.6	1.28	68.0	87.0	23.6	13,200	514	92	91
1.4	1.25	45.0	56.2	17.9	8,310	415	85	78
1.2	1.24	39.1	48.5	18.1	6,270	309	80	71
1.0	1.23	33.5	41.3	18.6	4,810	231	76	65
0.8	1.23	28.3	34.7	19.7	3,600	164	72	59
0.6	1.20	22.5	27.1	20.8	1,940	86	63	48

^a Polymer density was determined by a buoyancy method with hexane.

volume increase of the membrane upon absorption of an aqueous solution per cm³ of dry membrane [see eq (1)]; N_p is the number of ion-exchange sites in a cluster; and V_p is the volume of an ion-exchange (SO₃⁻) site (68×10^{-24} cm³).¹⁷ The number of ion-exchange sites per cluster, N_p , was obtained from the dry polymer density and the membrane IEC,

$$N_p = \left[\frac{N_A \rho_p (\text{IEC})}{1000 (1 + \Delta V)} \right] d^3 \quad (3)$$

where N_A is Avogadro's number, ρ_p is the dry polymer density, and IEC has units of mmol/g of dry membrane.

Cluster parameters for sulfonated PBMP membranes, equilibrated in 25°C water, with an IEC of between 0.6 mmol/g and 1.6 mmol/g, are listed in Table II, along with the number of water molecules per sulfonate site and the number of water molecules per cluster (based on 18 cm³/mol for the

partial molar volume of water). The cluster size, the number of charges per cluster, and the number of H₂O molecules per cluster increased with polymer IEC. Moreover, the difference between the Bragg spacing and the cluster size (i.e., the distance between two connected cluster boundaries) decreased with increasing IEC. The waters per cluster increase faster with IEC than the % macroscopic volume gain of the polymer; thus, there must be fewer but larger clusters in the high IEC membranes. Also, the number of waters per sulfonate site decreased with increasing IEC, up to a membrane ion-exchange capacity of 1.4 mmol/g; this trend was not observed in Nafion cation-exchange membranes.¹⁷ The effect of membrane water content on the Bragg spacing, cluster diameter, sulfonate charges per cluster, and other morphological parameters for a 1.2 mmol/g IEC sulfonated PBMP membrane (with no crosslinking) are listed in Table III. As expected, and in accordance with the result listed in Table II, both

Table III Microstructure Parameters for a 1.2 mmol/g Sulfonated PBMP Membrane (Noncrosslinked) at Different Degrees of Hydration (Temperature = 25°C)

Mass Gain, W (%)	Volume Gain, ΔV (%)	H ₂ O/SO ₃ H	H ₂ O/Cluster	Charge/Cluster	Bragg Spacing (Å)	Cluster Diameter (Å)
5.0	6.2	2.3	140	30	33	20
10.0	12.4	4.6	274	37	36	25
15.0	18.6	6.9	574	69	43	32
20.0	24.8	9.3	1,210	101	52	41
25.0	31.0	11.6	2,320	171	63	51
30.0	37.2	13.9	3,420	224	68	58
35.0	43.4	16.2	5,040	274	76	66
39.1	48.5	18.1	6,270	309	80	71

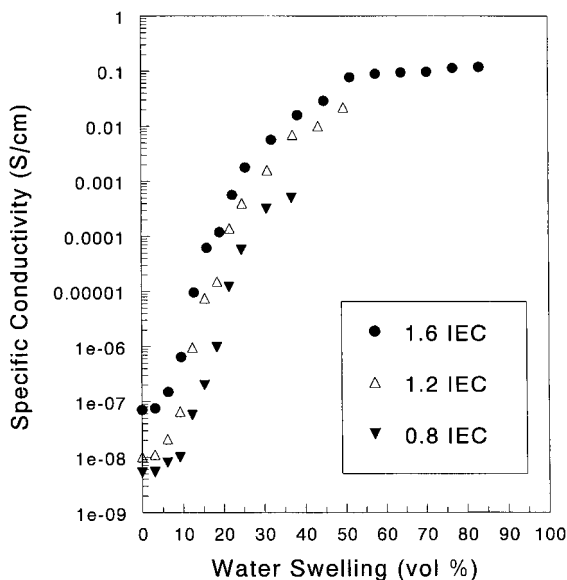


Figure 11 Dependence of proton conductivity on membrane water content at 25°C for sulfonated/noncrosslinked poly[bis(3-methylphenoxy)phosphazene] films.

the cluster size and SO_3^- charges per cluster increased with swelling. The increase in the number of ion-exchange sites per cluster with increasing water sorption suggests that cluster growth occurred by a combination of cluster expansion and a reorganization of sulfonate sites where the number of clusters decreased with increasing water swelling.

The cluster size for all of the sulfonated PBMP membranes in Table II was much larger than that in a water-equilibrated 0.909 mmol/g IEC Nafion 117 film (55 Å), suggesting that ionic sites can aggregate more easily in the polyphosphazene membranes. We have attributed this finding to: (i) The low glass transition temperature of the sulfonated PBMP membranes (ranging from about -5 to -10°C ,¹¹ compared to 110°C for Nafion 117¹⁸), and (ii) the absence of a three-dimensional crystal structure in the sulfonated PBMP polymer (whereas the perfluorosulfonic acid polymer of Nafion is 15–20% crystalline¹⁹).

Specific Proton Conductivity of Sulfonated PBMP Polymers

The effect of water content on the proton conductivity of sulfonated PBMP membranes (noncrosslinked) with an IEC of 0.8, 1.2, and 1.6 mmol/g is shown in Figure 11. At low water contents (<5%), the conductivity of all three films

was very low ($<1 \times 10^{-7}$ S/cm) and approximated that of the completely dry polymers. When the water content reached a value of about 15–25 vol %, the proton conductivity increased abruptly, with essentially no further change in conductivity when the polymer swelling exceeded 30 vol % (for the 0.8 IEC membrane) or 50 vol % (for the 1.2 and 1.6 IEC films). At a given degree of water swelling, the proton conductivity increased with increasing IEC, with a conductivity as high as 0.1 S/cm for the 1.6 mmol/g polymer, indicating that sulfonated polyphosphazenes are good proton conductors (comparable to Nafion) when swollen in water. As seen in Figure 11, there appears to be a percolation threshold, at which the conductivity abruptly increased with water sorption. To pursue this point further, the conductivity (κ) data in Figure 11 were fitted to the following power law percolation equation,

$$\kappa = \kappa_o(C - C_o)^n \quad (4)$$

where C is the volume fraction of water in the membrane [by definition, $C = \Delta V/(1 + \Delta V)$, with ΔV given by eq. (1)], C_o is the percolation threshold volume fraction, and κ_o and n are constants. When fitted to eq. (4), the 1.6, 1.2, and 0.8 IEC membrane conductivities fell on a single straight line as shown by the $\log \kappa$ vs. $\log(C - C_o)$ plot in Figure 12. The value of C_o for the three membranes was not the same (as is obvious from Fig. 11), but increased with decreasing IEC, where C_o was set equal to 0.175 (for the 1.6 IEC membrane), 0.20 (1.2 IEC), and 0.25 (0.8 IEC). These values of C_o are larger than that for Nafion (where $C_o = 0.10$ ²⁰) and indicate that the ionic clusters in the PBMP membranes aggregate into isolated regions, with the extent of isolation increasing with decreasing ion-exchange capacity. From a least-squares fit of the data, we found that $n = 1.26$ and $\kappa_o = 0.16$. The exponent value of 1.26 is consistent with that reported in the literature for a three-dimensional network of ionic clusters, and is similar to that found for a Nafion perfluorosulfonic acid membrane ($n = 1.5$).²⁰

The effect of temperature on proton conductivity for fully hydrated 1.2 mmol/g crosslinked and noncrosslinked PBMP membranes (in the H^+ form) is shown in Figure 13. The conductivities for both crosslinked and noncrosslinked polymers increased with temperature and displayed classical Arrhenius behavior, but the conductivity of the noncrosslinked film was more sensitive to

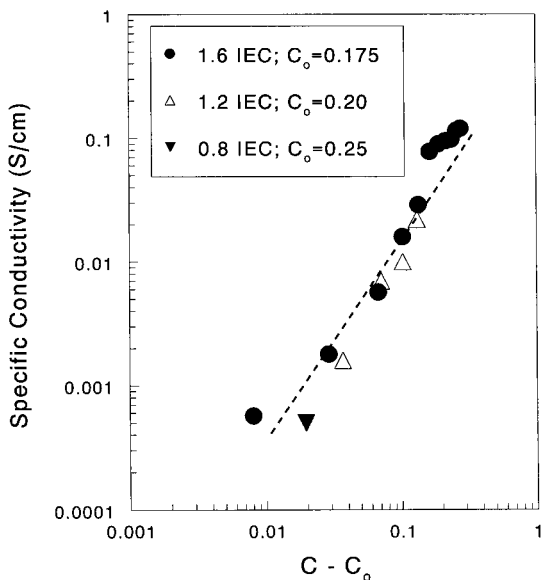


Figure 12 Log-log plot of proton conductivity vs. excess volume fraction of the sorbed aqueous phase for three sulfonated/non-crosslinked poly[bis(3-methylphenoxy)phosphazene] membranes.

temperature than its crosslinked counterpart. The increase in conductivity with temperature was due to the combined effects of more facile H^+ transport and an increase in membrane water content. The relationship between proton conductivity (κ) and temperature, was expressed by the Arrhenius equation,

$$\kappa = A \exp\left[-\frac{E_a}{RT}\right] \quad (5)$$

where A , E_a , R , and T denote the frequency factor, activation energy for ionic conductivity, gas constant, and temperature, respectively. The apparent activation energy for proton conduction was 36.7 kJ/mol for the noncrosslinked PBMP polymer and 27.8 kJ/mol for the crosslinked membrane, suggesting that proton migration in the PBMP membranes was primarily by the Grothuss mechanism.²¹ These apparent activation energies for proton conduction are considerably larger than that of Nafion (13.5 kJ/mol for Nafion 117²²), which we attributed to the strong temperature-dependence on water sorption by the PBMP membranes, especially for the noncrosslinked membrane.

CONCLUSIONS

Wide- and small-angle X-ray diffraction results indicated the presence of two phases in sulfonated

poly[bis(3-methylphenoxy)phosphazene] membranes—an amorphous phase and a two-dimensional ordered phase. The 2D structure changed, depending on the polymer's ion-exchange capacity and extent of water swelling, but the ionic fixed-charge groups did not completely disrupt the ordered morphology. The appearance of a reflection peak in small-angle X-ray scattering scans of dry and hydrated polymers with an ion-exchange capacity ≥ 0.6 mmol/g was evidence of ion clustering. The apparent Bragg spacing was about 30 Å for nonhydrated (dry) polymers of varying ion-exchange capacity (IEC) and varied from 50 to 90 Å for water-equilibrated membranes. For hydrated films, the cluster size increased with both IEC and the extent of water swelling but decreased with the weight of the cation associated with the SO_3^- fixed-charge sites. The specific conductivity of sulfonated membranes increased with polymer IEC and with the degree of polymer swelling. From the variation of conductivity with water content at 25°C, the percolation threshold porosity for sulfonated PBMP polymers varied from 0.175 (for a 1.6 mmol/g IEC membrane) to 0.25 (when the membrane IEC was 0.8 mmol/g), which was larger than the 0.10 threshold limit for a Nafion 117 perfluorosulfonic acid cation-exchange membrane. The apparent activation en-

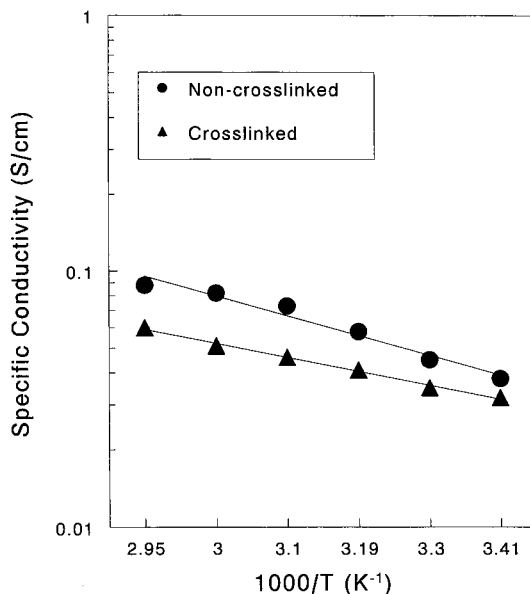


Figure 13 Effect of temperature on proton conductivity for water-equilibrated noncrosslinked and crosslinked (15 wt % benzophenone) poly[bis(3-methylphenoxy)phosphazene] membranes, with an IEC of 1.2 mmol/g.

ergies for proton conduction in a fully hydrated PBMP membrane (1.2 mmol/g IEC) was 36.7 kJ/mol (noncrosslinked) and 27.8 kJ/mol (for the crosslinked polymer), which is considerably larger than that for Nafion.

This work was supported by the Army Research Office, Grant No. DAAG55-98-1-0377, and by the National Science Foundation, Grant No. CTS-9632079.

REFERENCES

- Dotson, R. L.; Woodard, K. E. In *Perfluorinated Ionomer Membranes*; American Chemical Society Symposium Series 180; Eisenberg, A.; Yeager, H. L., Eds.; American Chemical Society: Washington, DC, 1982; p 311.
- Yeo, R. S.; Chin, D. T. *J Electrochem Soc* 1980, 127, 546.
- Gottesfeld, S.; Halpert, G.; Landgrebe, A. In *Proton Conducting Membrane Fuel Cells 1*; Electrochemical Society Proceedings PV 95-23; The Electrochemical Society: Pennington, NJ, 1996.
- MacKnight, W. J.; Taggart, W. P.; Stein, R. S. *J Polym Sci Polym Symp* 1974, 45, 113.
- Marx, C. L.; Caulfield, D. F.; Cooper, S. L. *Macromolecules* 1973, 6, 344.
- Dreyfus, B. *Macromolecules* 1985, 18, 284.
- Fujimura, M.; Hashimoto, T.; Kawai, H. *Macromolecules* 1982, 15, 136.
- Gierke, T. D.; Munn, G. E.; Wilson, F. C. *J Polym Sci Polym Phys Ed* 1981, 19, 1687.
- Gebel, G.; Lambard, J. *Macromolecules* 1997, 30, 7914.
- Capeci, S. W.; Pintauro, P. N.; Bennion, D. N. *J Electrochem Soc* 1989, 136, 2876.
- Tang, H.; Pintauro, P. N.; Guo, Q.; O'Connor, S. *J Appl Polym Sci* 1999, 71, 387.
- Guo, Q.; Pintauro, P. N.; Tang, H.; O'Connor, S. *J Membr Sci* 1999, 154, 175.
- Wycisk, R.; Pintauro, P. N.; Wang, W.; O'Connor, S. *J Appl Polym Sci* 1996, 59, 1607.
- Graves, R.; Pintauro, P. N. *J Appl Polym Sci* 1998, 68, 827.
- Zawodzinski, T. A.; Neeman, M.; Sillerud, L. O.; Gottesfeld, S. *J Phys Chem* 1991, 95, 6040.
- Hashimoto, T.; Fujimura, M.; Kawai, H. In *Perfluorinated Ionomer Membranes*; ACS Symposium Series No. 180; American Chemical Society: Washington, DC, 1982; p 217.
- Gierke, T. D.; Hsu, W. Y. In *Perfluorinated Ionomer Membranes*; ACS Symposium Series No. 180; American Chemical Society: Washington, DC, 1982; p 283.
- Yeo, S. C.; Eisenberg, A. *J Appl Polym Sci* 1977, 21, 875.
- Pineri, M.; Duplessix, R.; Volvino, F. In *Perfluorinated Ionomer Membranes*; ACS Symposium Series No. 180; American Chemical Society: Washington, DC, 1982; p 249.
- Hsu, W. Y.; Barkley, J. R.; Meakin, P. *Macromolecules* 1980, 13, 198.
- Sone, Y.; Ekdunge, P.; Simonsson, D. *J Electrochem Soc* 1996, 143, 1254.
- Halim, J.; Buchi, F. N.; Haas, O.; Stamm, M.; Scherer, G. G. *Electrochim Acta* 1994, 39, 1303.